Article

Journal of Vibration and Control
2020, Vol. 26(23–24) 2221–2229

DOI: 10.1177/1077546320916041
journals.sagepub.com/home/jvc
SAGE

Impact of losses on Love wave propagation in multilayered composite structures loaded with a Newtonian liquid

Kiełczyński Piotr, Marek Szalewski, Andrzej Balcerzak and Krzysztof Wieja

Abstract

In this study, we analyze theoretically and numerically the properties of Love surface waves propagating in lossy multilayered composite waveguides, loaded on the upper surface with a Newtonian liquid. The propagation of Love surface waves was formulated in terms of a direct Sturm–Liouville problem. An analytical form of the complex dispersion equation of the Love surface wave was derived using the Thomson–Haskell transfer matrix method. By separating the complex dispersion equation into its real and imaginary parts, we obtained a set of two nonlinear algebraic equations, which were subsequently solved numerically. The effect of various physical parameters of the lossy viscoelastic waveguide on the velocity and attenuation of the Love surface wave was then analyzed numerically. It was found that because of the presence of losses in the analyzed waveguide, Love surface waves displayed a number of new original phenomena, such as resonant-like maxima in attenuation as a function of thicknesses h_1 of the first viscoelastic surface layer and thickness h_2 of the second elastic surface layer. These phenomena are completely absent in lossless waveguides.

Keywords

Lossy waveguides, nondestructive testing of polymeric layered structures, Love surface waves, viscoelastic materials

1. Introduction

The propagation of elastic waves in layered structures was the subject of numerous theoretical and experimental investigations in recent decades (Achenbach, 1973; Auld, 1990; Royer and Dieulesaint, 2000; Rose, 2014). The most important types of elastic waves are surface Rayleigh and Love waves, Lamb plate waves, and Stoneley interface waves. The above types of elastic waves are ubiquitous in seismology, geophysics, nondestructive testing (NDT), and sensors technology.

Surface waves of the Love type have a number of unique features, which differentiate them from other types of surface elastic waves. First, Love surface waves have only one shear horizontal (SH) component of vibrations. As a result, the amplitude of Love surface waves is only slightly affected by loading with a viscous liquid. Second, the energy of Love waves attains high densities in guiding surface layers. This property is crucial in successful development of Love wave sensors working generally in a liquid environment (Kiełczyński, 1997; Kiełczyński and Szalewski, 2011; Kiełczyński et al., 2012, 2014, 2015). Last but not least, the analytical formulas describing propagation of Love surface waves are relatively compact, which enable drawing clear physical conclusions.

In a vast majority of articles analyzing properties of Love surface waves in geophysics, sensors, and layered composite materials, Love wave waveguides were considered to be entirely lossless (Kakar and Kakar, 2012; Kundu et al., 2014; Singh, 2010). However, real Love wave waveguides have to be necessarily lossy because of the inherent viscoelastic properties of the constituent materials, and an extra loading with a viscous liquid, in the case of sensors.

The main purpose of this work is to overcome the limitations of existing theories by extending the analysis to the case of Love wave propagation in lossy multilayered composite waveguides. Needless to say, introduction of losses will complicate significantly the corresponding

Institute of Fundamental Technological Research, Polish Academy of Sciences, Poland

Received: 30 July 2019; accepted: 5 March 2020

Corresponding author:
Kiełczyński Piotr, Institute of Fundamental Technological Research, Polish Academy of Sciences, ul. Pawińskiego 5B, 02-106 Warsaw, Poland.
Email: pkielczy@ippt.pan.pl

analysis. However, more importantly, it will reveal new phenomena, which are completely absent in lossless waveguides. As a matter of fact, the propagation of elastic surface waves in the lossy media has been only addressed in a limited number of works (Chattopadhyay et al., 2010; Guo and Sun, 2008; Kiełczyński, 2018; Sharma and Kumar, 2017; Yuan et al., 2019).

In this study, we analyze theoretically the properties of SH surface waves of the Love type, propagating in lossy, composite waveguides consisting of two surface layers deposited on an elastic substrate. First surface layer no. 1 (looking from the top) is a lossy, viscoelastic layer, described by the Kelvin–Voigt rheological model. Second lossless elastic surface layer no. 2 is sandwiched between the first lossy surface layer and the lossless semi-infinite elastic substrate (material no. 3). The first lossy surface layer of the waveguide is additionally loaded with a lossy Newtonian viscous liquid (material no. 0) of an infinite thickness.

In Section 3, we established an analytical form of the complex dispersion equation for the Love wave using the Thomson–Haskell transfer matrix method.

The phase velocity and attenuation of Love surface waves propagating in the analyzed lossy multilayer waveguide, loaded with a Newtonian liquid, were calculated numerically (by solving the dispersion equation) in Section 4 as a function of various physical parameters of the composite layered viscoelastic waveguide, such as thickness h_1 and viscosity η_{44} of the first viscoelastic surface layer, viscosity η of the loading Newtonian liquid, and thickness h_2 of the second lossless elastic surface layer.

In Section 5, discussion of the obtained results is presented, and in Section 6, conclusions and possible potential applications are established.

This study may be of interest for engineers and scientists working in NDT of composite materials used in aerospace technology, rheology of materials, seismology, and the design and optimization of biosensors and chemosensors.

2. Mathematical formulation of the problem: direct Sturm–Liouville problem

The propagation of Love surface waves in multilayered composite waveguides, with known material and geometric parameters, can be formulated in terms of the direct Sturm–Liouville problem (Kiełczyński, 2018). Solutions to this direct Sturm–Liouville problem form a set of discrete eigenvalue–eigenvector pairs. An eigenvalue corresponds to the complex wave vector k , comprising the phase velocity v_p and attenuation α of the Love wave. The associated eigenvector describes spatial distribution of the mechanical displacement of the Love surface wave as a function of depth x_2, that is the direction normal to the guiding surface $x_2 = 0$ (see Figure 1).

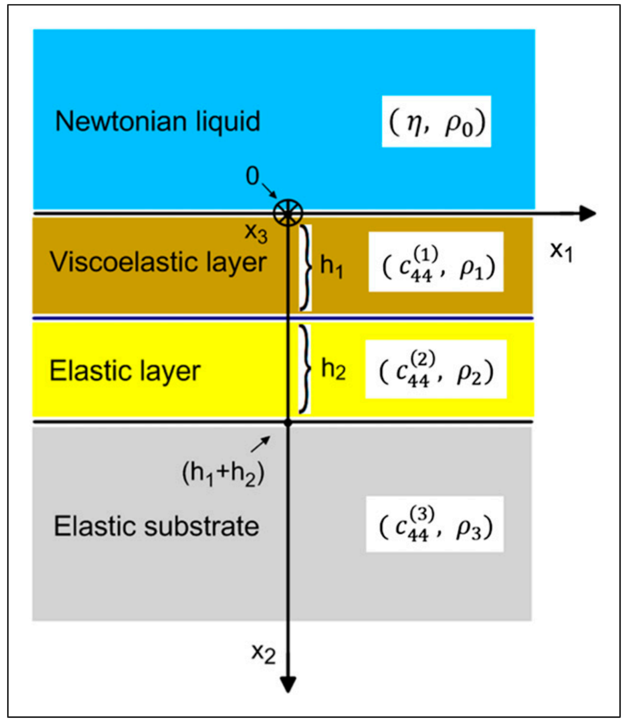

Figure 1. Cross section of the analyzed lossy multilayered composite Love wave waveguide. Love surface waves propagate along the x_1 axis. Shear horizontal mechanical displacement u_3 of the Love wave is directed along the x_3 axis. Newtonian liquid (material no. 0) and first surface layer no. 1 are lossy. Second surface layer no. 2 and the substrate (material no. 3) are lossless.

Because the layered composite waveguide is lossy, the wave number k of the Love wave is necessarily a complex quantity

$$k = k_0 + j\alpha \tag{1}$$

where $j = \sqrt{-1}$ is the imaginary unit.

The real part (k_0) of the complex wave number k determines the phase velocity of the Love wave $v_p = \omega/k_0$, where ω is the angular frequency of the wave. On the other hand, the imaginary part α of the wave number k is the coefficient of attenuation of the Love wave.

2.1. Geometry and material parameters of the lossy composite Love wave waveguide

The multilayered viscoelastic composite waveguide structure analyzed in this study is shown in Figure 1. The composite waveguide consists of first viscoelastic (Kelvin–Voigt type) surface layer no. 1 $(0 < x_2 \le h_1)$ deposited on second lossless elastic surface layer no. 2 $(h_1 < x_2 \le h_2 + h_1)$, which in turn is rigidly bonded to an infinite elastic substrate (material no. 3), occupying the lower half-space $(x_2 > h_2 + h_1)$. In addition, the top surface of surface layer no. 1 $(x_2 = 0)$ is loaded with an infinite viscous

(Newtonian) liquid (material no. 0), occupying the lower half-space ($x_2 < 0$). The Newtonian liquid is characterized by its viscosity η and density ρ_0 as well as by the complex shear modulus of elasticity $c_{44}^{(0)} = -j\omega\eta$. It is assumed that SH surface waves of the Love type propagate in direction x_1 in the analyzed waveguide structure.

Viscoelastic properties of first lossy surface layer no. 1, made, for example of a poly(methyl methacrylate) (PMMA) material, are modeled by the Kelvin–Voigt (K–V) rheological model (Gutierrez-Lemini, 2014). According to the Kelvin–Voigt rheological model, the complex shear modulus of elasticity $c_{44}^{(1)}$ of the PMMA material constituting first surface layer no. 1 is given by the following formula

$$c_{44}^{(1)} = c_1 - j\omega\eta_{44} \tag{2}$$

where c_1 is the shear storage modulus of elasticity, η_{44} is the viscosity of the material, and ω is the angular frequency ($\omega = 2\pi \cdot f$).

Second surface layer no. 2 is a lossless elastic material (such as gold (Au)), with a real shear modulus of elasticity $c_{44}^{(2)}$. The elastic substrate (such as ST-cut quartz supporting pure SH bulk waves) is a semi-infinite elastic material (no. 3) with a real shear modulus of elasticity equal to $c_{44}^{(3)}$. The axis x_2 is directed into the bulk of the substrate. In addition, all material parameters of the composite waveguide are homogeneous along x_1 and x_3 axes and change only along the x_2 axis.

3. Complex dispersion equation of the Love surface wave

3.1. Governing equations of motion

3.1.1. Semi-infinitive layer of Newtonian liquid ($x_2 < 0$). The mechanical displacement $u_3^{(0)}$ of the bulk SH wave (generated by the Love surface wave) is governed by the following Navier–Stokes partial differential equation

$$\frac{\partial^2 u_3^{(0)}}{\partial t^2} = \left(\frac{-j\omega\eta}{\rho_1}\right)\left(\frac{\partial^2 u_3^{(0)}}{\partial x_1^2} + \frac{\partial^2 u_3^{(0)}}{\partial x_2^2}\right) \tag{3}$$

where ρ_1 is the liquid density, η is the viscosity, and ω is the angular frequency of the Love wave.

3.1.2. Lossy viscoelastic surface layer ($h_1 > x_2 > 0$). The mechanical displacement $u_3^{(1)}$ of the Love wave in the viscoelastic surface layer fulfills the following equation of motion

$$\frac{1}{v_1^2}\frac{\partial^2 u_3^{(1)}}{\partial t^2} = \frac{\partial^2 u_3^{(1)}}{\partial x_1^2} + \frac{\partial^2 u_3^{(1)}}{\partial x_2^2} \tag{4}$$

where $v_1 = ((c_0 - j\omega\eta_{44})/\rho_1)^{1/2} = v_1^0(1 - (j\omega\eta_{44}/c_0))^{1/2}$ is the complex bulk SH wave velocity in the first viscoelastic surface layer, c_0 is the storage modulus, ρ_1 is the density of the viscoelastic surface layer, and η_{44} is the viscosity.

3.1.3. Lossless elastic subsurface layer ($h_1 > x_2 > h_1 + h_2$). The mechanical displacement $u_3^{(2)}$ of the Love wave in the elastic subsurface layer is governed by the following equation of motion

$$\frac{1}{v_2^2}\frac{\partial^2 u_3^{(2)}}{\partial t^2} = \frac{\partial^2 u_3^{(2)}}{\partial x_1^2} + \frac{\partial^2 u_3^{(2)}}{\partial x_2^2} \tag{5}$$

where $v_2 = (c_{44}^{(2)}/\rho_2)^{1/2}$ is the bulk SH wave velocity in the lossless subsurface layer, $c_{44}^{(2)}$ is the storage modulus of elasticity, and ρ_2 is the density of the lossless elastic subsurface layer.

3.1.4. Semi-infinitive elastic substrate ($x_2 > h_1 + h_2$). The mechanical displacement $u_3^{(3)}$ of the Love wave in the elastic substrate satisfies the following partial differential equation (equation of motion)

$$\frac{1}{v_3^2}\frac{\partial^2 u_3^{(3)}}{\partial t^2} = \frac{\partial^2 u_3^{(3)}}{\partial x_1^2} + \frac{\partial^2 u_3^{(3)}}{\partial x_2^2} \tag{6}$$

where $v_3 = (c_{44}^{(3)}/\rho_3)^{1/2}$ is the velocity of the bulk SH wave in the elastic substrate, $c_{44}^{(3)}$ is the storage modulus of elasticity, and ρ_3 is the density in the elastic substrate.

3.2. Thomson–Haskell transfer matrix method

The complex dispersion equation of Love surface waves propagating in the lossy waveguide presented in Figure 1 has been derived in this article using the Thomson–Haskell transfer matrix method (Haskell, 1953; Ke et al., 2011; Thomson, 1950).

The key element in the Thomson–Haskell method is to relate mechanical displacement and shear stress of the Love wave on the upper surface of each layer with mechanical displacement and shear stress on the lower surface of the considered layer. Below we show briefly the derivation of this relationship.

A general form of the time-harmonic solution for the equations of motion (equations (3)–(6)) in the subsequent layers corresponding to a time-harmonic Love surface wave is sought in the following form

$$u_3(x_1, x_2, t) = V(x_2) \cdot \exp[j(kx_1 - \omega t)] \tag{7}$$

where $V(x_2)$ is the transverse distribution of the mechanical displacement u_3 of the Love surface wave as a function of depth x_2.

The shear stress associated with the mechanical displacement u_3 of the Love wave is given by the following formula

$$\tau_{23}(x_1, x_2, t) = T(x_2) \cdot \exp[j(kx_1 - \omega t)] \tag{8}$$

where $T(x_2) = c_{44}(x_2)(\partial V(x_2)/\partial x_2)$. Here, $c_{44}(x_2)$ is the shear modulus of elasticity of the material in the constituent parts of the waveguide.

The equation of motion (see equations (3)–(6)) for the subsequent layer is an ordinary differential equation of second order. Considering two new dependent variables (V and T), each of the second order differential equations (3)–(6) can be represented as a system of two differential equations of the first order, namely

$$\frac{d}{dx}\begin{bmatrix} V \\ T \end{bmatrix} = [A]\begin{bmatrix} V \\ T \end{bmatrix} = \begin{bmatrix} 0 & \frac{1}{c_{44}(x)} \\ \beta^2 c_{44}(x) - \omega^2 \rho(x) & 0 \end{bmatrix}\begin{bmatrix} V \\ T \end{bmatrix} \tag{9}$$

Solving this matrix differential equation (9), for example for the PMMA surface layer, we arrive at the following formula (equation (10)) linking mechanical displacement and shear stress on the upper surface of the PMMA layer for ($x_2 = 0$) with mechanical displacement and shear stress on the lower surface of this layer for ($x_2 = h_1$). Details of this derivation are given in Kiełczyński et at., (2016)

$$\begin{bmatrix} V \\ T \end{bmatrix}\Bigg|_{x=h_1} = \cos(q_1 \cdot h_1) \times \begin{bmatrix} 1 & \frac{1}{c_{44}^{(1)} \cdot q_1}\tan(q_1 \cdot h_1) \\ -c_{44}^{(1)} \cdot q_1 \cdot \tan(q_1 \cdot h_1) & 1 \end{bmatrix} \times \begin{bmatrix} V \\ T \end{bmatrix}\Bigg|_{x=0} \tag{10}$$

where $q_1 = \sqrt{k_1^2 - k^2}$ is the transverse wave number of the Love wave in the first PMMA surface layer, $k_1 = (\omega/v_1)$ is the wave number of bulk SH waves in the PMMA surface layer, $v_1 = (c_{44}^{(2)}/\rho_1)^{1/2}$ is the phase velocity of bulk SH waves in the PMMA surface layer, and $k = k_0 + j\alpha$ is the complex wave number of the Love wave.

For a two-layer ($N = 2$) system (PMMA surface layer no. 1 deposited on second surface Au layer no. 2, see Figure 1), the dependence between the mechanical displacement and the shear stress on the lower (bottom) surface of the second elastic surface layer no. 2 (Au) $x_2 = (h_1 + h_2)$ and on the upper ($x_2 = 0$) surface of the first viscoelastic PMMA surface layer no. 1 is given by a resulting transfer matrix $[A]$, being a product of two matrices (10) written for the surface layer no. 1 and layer no. 2, respectively, that is

$$[A] = M \times \begin{bmatrix} 1 & \frac{1}{c_{44}^{(2)} \cdot q_2}\tan(q_2 \cdot h_2) \\ -c_{44}^{(2)} \cdot q_2 \cdot \tan(q_2 \cdot h_2) & 1 \end{bmatrix} \times \begin{bmatrix} 1 & \frac{1}{c_{44}^{(1)} \cdot q_1}\tan(q_1 \cdot h_1) \\ -c_{44}^{(1)} \cdot q_1 \cdot \tan(q_1 \cdot h_1) & 1 \end{bmatrix} \tag{11}$$

where $M = \cos(q_2 \cdot h_2)\cos(q_1 \cdot h_1), q_2 = \sqrt{k_2^2 - k^2}, k_2^2 = (\omega^2/v_2^2)$, and $v_2 = (c_{44}^{(2)}/\rho_2)^{1/2}$.

Having performed the corresponding multiplications, equation (11) leads to the following expression for the overall transfer matrix $[A]$

$$[A] = \begin{bmatrix} A_{11} & A_{12} \\ A_{21} & A_{22} \end{bmatrix} = M \times \begin{bmatrix} B_{11} & B_{12} \\ B_{21} & B_{22} \end{bmatrix} \tag{12}$$

where $B_{11} = 1 - \tan(q_1 \cdot h_1) \cdot \tan(q_2 \cdot h_2) \cdot \{(c_{44}^{(1)} \cdot q_1 / c_{44}^{(2)} \cdot q_2)\}$, $B_{12} = (1/c_{44}^{(1)} \cdot q_1)\tan(q_1 \cdot h_1) + (1/c_{44}^{(2)} \cdot q_2)\tan(q_2 \cdot h_2)$, $B_{21} = -c_{44}^{(2)} \cdot q_2 \cdot \tan(q_2 \cdot h_2) - c_{44}^{(1)} \cdot q_1 \cdot \tan(q_1 \cdot h_1)$, $B_{22} = 1 - \tan(q_1 \cdot h_1) \cdot \tan(q_2 \cdot h_2) \cdot \{(c_{44}^{(2)} \cdot q_2 / c_{44}^{(1)} \cdot q_1)\}$

The unknown components of the mechanical displacement and the corresponding shear stress of the Love wave at the interface $x_2 = 0$ and $x_2 = h_1 + h_2$ will be further denoted by V_0, T_0 and V_D, T_D, respectively

$$\begin{bmatrix} V_D \\ T_D \end{bmatrix} = \begin{bmatrix} A_{11} & A_{12} \\ A_{21} & A_{22} \end{bmatrix}\begin{bmatrix} V_0 \\ T_0 \end{bmatrix} \tag{13}$$

3.3. Shear stresses on top of the first surface layer no 1 and bottom of the second surface layer no 2

The top surface of first PMMA layer no. 1 ($x_2 = 0$) is loaded with a semi-infinite Newtonian liquid. The dependence of the mechanical displacement on the depth $V(x_2)$ in the Newtonian liquid is given by $V(x_2) = V_0 \cdot \exp(\lambda_1 \cdot x_2)$. Thus, the shear stress of the bulk SH wave in a Newtonian liquid at the interface with PMMA surface layer no. 1 is given by

$$T_0 = c_{44}^{(0)} \frac{\partial V}{\partial x_2}\bigg|_{x_2=0} = c_{44}^{(0)} \cdot \lambda_1 \cdot V_0 \tag{14}$$

where $c_{44}^{(0)} = -j\omega\eta$ is a complex shear modulus of elasticity of the Newtonian liquid, $\lambda_1 = (k^2 - k_0^2)^{1/2}$, and $k_0^2 = j\omega(\rho_l/\eta)$. The parameters λ_1 and k_0 correspond, respectively, to the transverse wave number of the Love surface wave in the Newtonian liquid and the complex wave number of bulk SH waves in the Newtonian liquid.

Bottom of the elastic surface layer no. 2 (Au) ($x_2 = h_1 + h_2$) is rigidly bonded to the semi-infinite elastic substrate (material no. 3). The dependence of the mechanical displacement on the depth $V(x_2)$ in an elastic substrate is given by $V(x_2) = V_D \cdot \exp(-b \cdot x_2)$. Therefore, the shear stress in the elastic substrate at the interface with elastic surface layer no. 2 (Au) is given by

$$T_D = c_{44}^{(3)} \frac{\partial V}{\partial x_2}\bigg|_{x_2=(h_1+h_2)} = -c_{44}^{(3)} \cdot b \cdot V_D \tag{15}$$

where $b = (k^2 - k_3^2)^{1/2}$, $k_3 = (\omega/v_3)$, and $v_3 = (c_{44}^{(3)}/\rho_3)^{1/2}$. The parameters b and k_3 correspond, respectively, to the transverse wave number of the Love surface wave in the substrate and the wave number of bulk SH waves in the substrate.

Substituting values of the shear stresses T_0 and T_D given by equations (14) and (15) into (13) leads to

$$\begin{bmatrix} V_D \\ -c_{44}^{(3)} \cdot b \cdot V_D \end{bmatrix}\Bigg|_{x=(h_1+h_2)} = \begin{bmatrix} A_{11} & A_{12} \\ A_{21} & A_{22} \end{bmatrix} \begin{bmatrix} V_0 \\ c_{44}^{(0)} \cdot \lambda_1 \cdot V_0 \end{bmatrix}\Bigg|_{x=0} \tag{16}$$

In fact, equation (16) contains only two unknowns, namely V_0 and V_D. By a simple rearrangement of the terms, equation (16) can be written as

$$\begin{bmatrix} 1 & -\left(A_{11} + A_{12} \cdot c_{44}^{(0)} \cdot \lambda_1\right) \\ c_{44}^{(3)} \cdot b & \left(A_{21} + A_{22} \cdot c_{44}^{(0)} \cdot \lambda_1\right) \end{bmatrix} \begin{bmatrix} V_0 \\ V_D \end{bmatrix} = \begin{bmatrix} 0 \\ 0 \end{bmatrix} \tag{17}$$

3.4. Determination of the complex dispersion equation

A necessary condition for the existence of a nonzero solution of equation (17) requires zeroing of the determinant of the 2 × 2 matrix in equation (17). This condition leads to the following complex dispersion equation for Love waves

$$\left(A_{21} + A_{22} \cdot c_{44}^{(0)} \cdot \lambda_1\right) + \left(c_{44}^{(3)} \cdot b\right)\left(A_{11} + A_{12} \cdot c_{44}^{(0)} \cdot \lambda_1\right) = 0 \tag{18}$$

Substituting into equation (18), the elements of the matrix $[A]$ given by equation (12), we arrive finally at the following complex dispersion equation for the Love surface waves propagating in the lossy composite waveguide, as shown in Figure 1

$$\begin{aligned} &-\tan(q_1 \cdot h_1) \cdot \tan(q_2 \cdot h_2) \left\{ \frac{\left(\lambda_1 \cdot c_{44}^{(0)}\right)}{\left(c_{44}^{(3)} \cdot b\right)} \frac{\left(c_{44}^{(2)} \cdot q_2\right)}{\left(c_{44}^{(1)} \cdot q_1\right)} \right. \\ &\left. + \frac{\left(c_{44}^{(1)} \cdot q_1\right)}{\left(c_{44}^{(2)} \cdot q_2\right)} \right\} + \tan(q_1 \cdot h_1) \left\{ \frac{\left(\lambda_1 \cdot c_{44}^{(0)}\right)}{\left(c_{44}^{(1)} \cdot q_1\right)} \right. \\ &\left. - \frac{\left(c_{44}^{(1)} \cdot q_1\right)}{\left(c_{44}^{(3)} \cdot b\right)} \right\} + \tan(q_2 \cdot h_2) \left\{ \frac{\left(\lambda_1 \cdot c_{44}^{(0)}\right)}{\left(c_{44}^{(2)} \cdot q_2\right)} \right. \\ &\left. - \frac{\left(c_{44}^{(2)} \cdot q_2\right)}{\left(c_{44}^{(3)} \cdot b\right)} \right\} + \left(\frac{\left(\lambda_1 \cdot c_{44}^{(0)}\right)}{\left(c_{44}^{(3)} \cdot b\right)} + 1 \right) = 0 \end{aligned} \tag{19}$$

Despite being complex, the dispersion equation (19) contains only two real-valued unknowns, that is the real k_0 and imaginary α parts of the complex wave number k of the Love wave (see equation (1)).

The complex dispersion equation, equation (19), can be subsequently split into its real $Re\,\boldsymbol{F}$ and imaginary $Im\,\boldsymbol{F}$ parts, which we will equate simultaneously to zero, namely

$$Re\,\boldsymbol{F}\left(c_{44}^{(1)}, \rho_1, c_{44}^{(2)}, \rho_2, c_{44}^{(3)}, \rho_3, \eta, \rho_l, \eta_{44}, h_1, h_2, \omega; k_0, \alpha\right) = 0 \tag{20}$$

$$Im\,\boldsymbol{F}\left(c_{44}^{(1)}, \rho_1, c_{44}^{(2)}, \rho_2, c_{44}^{(3)}, \rho_3, \eta, \rho_l, \eta_{44}, h_1, h_2, \omega; k_0, \alpha\right) = 0 \tag{21}$$

Equations (20) and (21) constitute a system of two nonlinear, transcendental algebraic equations for two real unknowns k_0 and α. The parameters included explicitly in equations (20) and (21) are the following $c_{44}^{(1)}, \rho_1, c_{44}^{(2)}, \rho_2, c_{44}^{(3)}, \rho_3, \eta, \rho_0, \eta_{44}, h_1, h_2$, and ω. The nonlinear system of two algebraic equations (20) and (21) has been solved numerically, using the adequate procedures provided by software package Scilab. If the values of k_0 and α are already determined, the phase velocity of the Love surface wave can be readily calculated from the following elementary formula $v_p = \omega/k_0$.

4. Results of numerical calculations

Numerical calculations were performed for Love surface waves propagating in the composite lossy waveguide structure (Figure 1), consisting of material and geometrical parameters of the multilayered composite waveguide, used in numerical calculations, which are given explicitly in Table 1.

Table 1. Material and geometrical parameters of the lossy multilayered Love wave waveguide (Figure 1) used in numerical calculations.

Material	Thickness (μm)	Density (kg/m^3)	Storage shear modulus (GPa)	Shear horizontal wave velocity (m/s)	Viscosity (Pa s)
Newtonian liquid	Semi-infinite	$\rho_0 = 1000$	0	NA	$\eta = 0$–200
PMMA surface layer	$h_1 = 0$–2000	$\rho_1 = 1180$	$c_1 = 1.43$	$v_1^0 = 1100$	$\eta_{44} = 0$–200
Gold subsurface layer	$h_2 = 0$–2000	$\rho_2 = 19300$	$c_{44}^{(2)} = 27.52$	$v_2 = 1194$	0
ST-cut quartz substrate	Semi-infinite	$\rho_3 = 2650$	$c_{44}^{(3)} = 67.85$	$v_3 = 5060$	0

Phase velocity v_p and attenuation α of the Love surface wave were determined as a function of the following parameters: (1) thickness h_1 of the first PMMA surface layer, (2) thickness h_2 of the second (Au) surface layer, and (3) wave frequency f. PMMA: poly(methyl methacrylate).

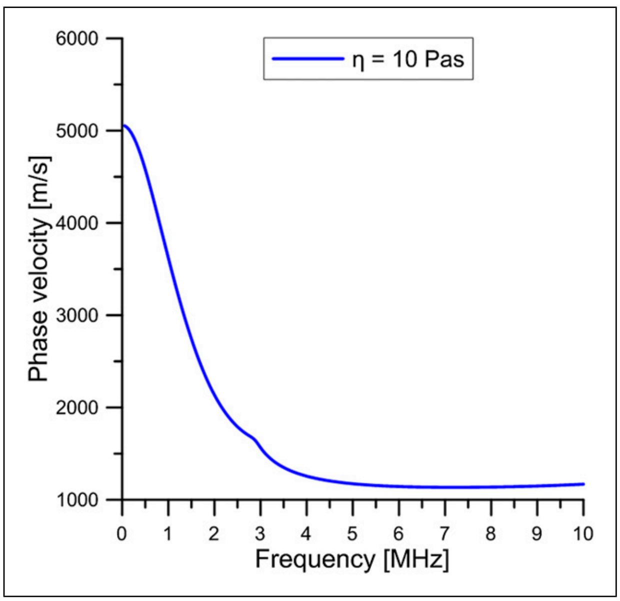

Figure 2. Phase velocity v_p of Love surface waves, as a function of frequency f, for the viscosity of the loading Newtonian liquid $\eta = 10$ Pa s. The viscosity of the first PMMA surface layer $\eta_{44} = 0.37$ Pa s. Thickness of the first PMMA surface layer $h_1 = 100$ μm. Thickness of the second elastic surface layer (Au) $h_2 = 100$ μm. PMMA: poly(methyl methacrylate).

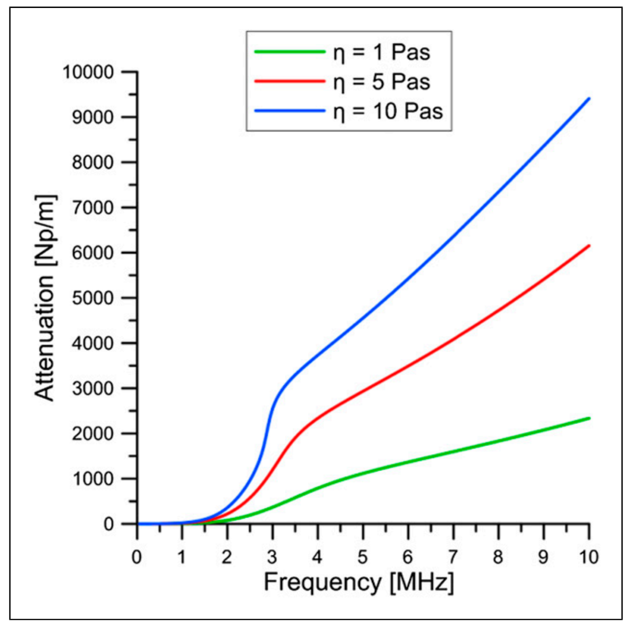

Figure 3. Attenuation α of Love surface waves, as a function of frequency f, for different values of viscosity η of the Newtonian liquid $\eta = 1, 5$, and 10 Pa s. Viscosity of the first PMMA surface layer $\eta_{44} = 0.37$ Pa s. Thickness of the first PMMA surface layer $h_1 = 100$ μm. Thickness of the second elastic (Au) surface layer $h_2 = 100$ μm. PMMA: poly(methyl methacrylate).

4.1. Phase velocity and attenuation of Love waves

The influence of the Newtonian liquid on the phase velocity of Love surface waves is in general small. Therefore, the phase velocity v_p is plotted in Figure 2 only for one viscosity of the Newtonian liquid, namely for $\eta = 10$ Pa s.

A small wrinkle in Figure 2, that occurs approximately at the same frequency ~2.8 MHz, as the inflection point in the attenuation of the Love wave (see Figure 3), can be considered as a secondary effect caused by high viscosity $\eta = 10$ Pa s of the loading viscoelastic liquid. In lossless waveguides, this small irregularity in the phase velocity vanishes.

In contrast to the phase velocity v_p, shown in Figure 2, the attenuation α of Love surface waves (see Figure 3) depends strongly on viscosity η of the loading Newtonian liquid.

At a frequency of ~2.8 MHz, the attenuation α of Love surface waves exhibits clear inflection point (see Figure 3). This phenomenon occurs approximately for the same value of the product $fh_1 \approx 280$ MHz μm and $fh_2 \approx 280$ MHz μm, as that at which we observe a resonant-like attenuation of the Love surface wave, as a function of thickness h_1 of the first PMMA surface layer (see Figure 5) and as a function of thickness h_2 of the second (Au) surface layer (see Figure 7).

If the thickness of the first PMMA surface layer equals zero $h_1 = 0$, Love surface waves are still guided by a remaining second (Au) surface layer of thickness $h_2 = 100\,\mu$m. However, if thickness $h_1 = 0$, the phase velocity v_p of Love surface waves equals approximately $v_p \approx 3750$ m/s, at a frequency 1 MHz (see Figure 4), and is a decreasing function of thickness h_1 of the first PMMA surface layer, as expected.

By contrast to the phase velocity v_p, the attenuation α of Love surface waves (Figure 5) displays resonant-like maxima, as a function of thickness h_1 of the first PMMA surface layer. The resonant-like maxima are located approximately at the vicinity of the steepest descent of the phase velocity, as a function of thickness h_1 of the first PMMA surface layer (see Figure 4), for the product $fh_1 \approx 280$ MHz µm (see Figure 5). PMMA: poly(methyl methacrylate).

The viscosity η of the loading Newtonian liquid has no influence on the phase velocity of Love surface waves, as a function of thickness h_2 of the second (Au) surface layer (Figure 6). However, the attenuation of Love waves is a pronounced function of thickness h_2 of the second buried elastic surface layer of and the viscosity η of the loading Newtonian liquid (Figure 7). In addition, the attenuation of Love surface waves displays resonant-like maxima, as a function of thickness h_2, with the amplitude proportional to $\sqrt{\eta}$.

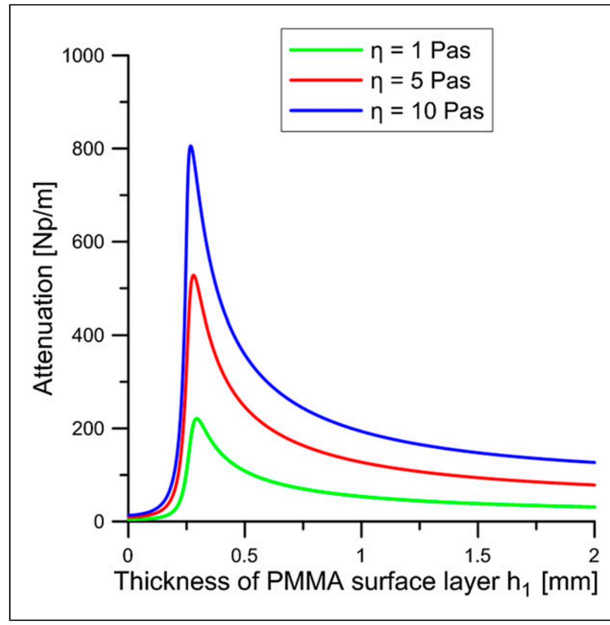

Figure 5. Attenuation α of Love surface waves, as a function of thickness h_1 of the first PMMA surface layer, for different values of viscosity $\eta = 1, 5$, and 10 Pa s of the loading Newtonian liquid. Viscosity of the first PMMA surface layer $\eta_{44} = 0.37$ Pa s. Thickness of the second elastic (Au) surface layer $h_2 = 100\,\mu$m. Frequency $f = 1$ MHz. PMMA: poly(methyl methacrylate).

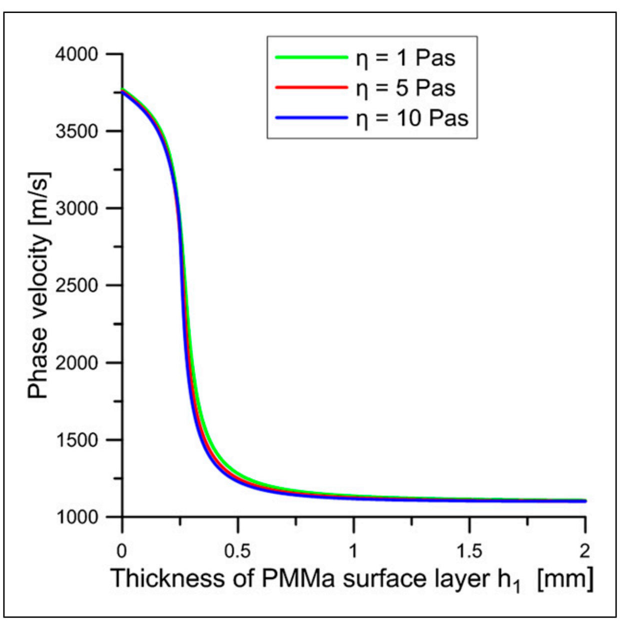

Figure 4. Phase velocity v_p of Love surface waves, as a function of thickness h_1 of the first PMMA surface layer, for different values of viscosity $\eta = 1,\ 5$, and 10 Pa s of the Newtonian liquid. The viscosity of the first PMMA surface layer $\eta_{44} = 0.37$ Pa s. Thickness of the second elastic (Au) surface layer $h_2 = 100\,\mu$m. Frequency of the Love wave $f = 1$ MHz. PMMA: poly(methyl methacrylate).

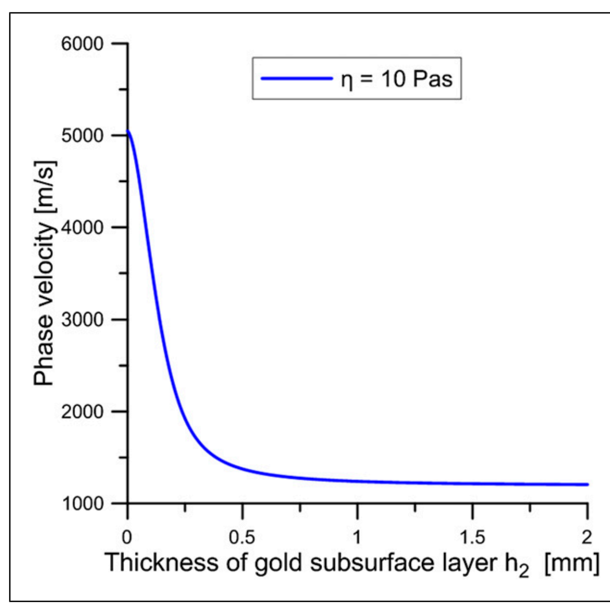

Figure 6. Phase velocity v_p of Love surface waves, as a function of thickness h_2 of the second elastic (Au) surface layer, for viscosity $\eta = 10$ Pa s of the loading Newtonian liquid. The viscosity of the first PMMA surface layer $\eta_{44} = 0.37$ Pa s. Thickness of the first PMMA surface layer $h_1 = 100\,\mu$m. Frequency $f = 1$ MHz. PMMA: poly(methyl methacrylate).

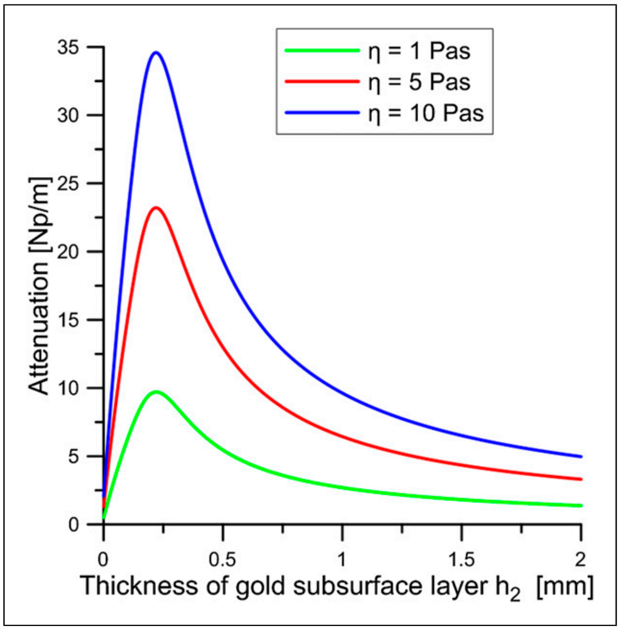

Figure 7. Attenuation α of Love surface waves, as a function of thickness h_2 of the second elastic (Au) surface layer, for different values of viscosity $\eta = 1, 5$, and 10 Pa s of the loading Newtonian liquid. The viscosity of the first PMMA surface layer $\eta_{44} = 0.37$ Pa s. Thickness of the first PMMA surface layer $h_1 = 100\,\mu$m. Frequency $f = 1$ MHz. PMMA: poly(methyl methacrylate).

The phase velocity of the Love wave as a function of thickness h_2 of the second elastic surface layer, for viscosities $\eta = 1$ and 5 Pa s of the loading Newtonian liquid, was almost identical to that corresponding to viscosity $\eta = 10$ Pa s, thus, it is not plotted in Figure 6.

5. Discussion

First, the new phenomenon, which we observed in lossy Love wave waveguides, analyzed in this paper, can be discerned from Figure 2 by tracing the phase velocity v_p of Love surface waves, as a function of frequency f. Initially, the phase velocity v_p drops quickly from $v_p = 5060$ m/s at $f \approx 0$ MHz to $v_p \approx 1100$ m/s at $f = 5$ MHz. Then, the phase velocity v_p attains a plateau and starts to increase for frequencies higher than ~7 MHz. The viscosity of the Newtonian liquids loading the waveguide in Figure 2 was $\eta = 10$ Pa s. Interestingly, an analogous phenomenon was not observed for lower viscosities ($\eta = 1$–5 Pa s) of the loading Newtonian liquid. The results presented in Figure 2 suggest that high viscosity η of the loading Newtonian liquid has in general a stiffening effect on overall properties of Love wave waveguides.

Second, a new phenomenon was observed in Figure 3 for the attenuation $\alpha(f)$ of Love surface waves, as a function of frequency f. At the beginning, the attenuation increases with frequency, then reaches an inflection point at $f = 2.8$ MHz, for $\eta = 10$ Pa s, and finally the attenuation grows almost linearly with the frequency. It is interesting to note that the inflection point in Figure 3 occurs for the product $fh_1 \approx 280$ MHz µm.

The attenuation α of Love surface waves, as a function of thickness of PMMA surface layer h_1 and thickness of gold layer h_2, grows with viscosity η of the loading Newtonian liquid approximately as $\sqrt{\eta}$ (see Figures 3, 5, and 7).

Next, the new important phenomenon discovered by the authors in this study is a resonant-like character of the attenuation α of Love surface waves as a function of thickness h_1 of the first lossy PMMA surface layer (see Figure 5) and thickness h_2 of the second lossless (Au) elastic surface layer (Figure 7). Interestingly enough, the second lossless gold surface layer (thickness h_2) can "see" losses of the loading Newtonian liquid (viscosity η), despite the fact that these two materials are physically separated by an intermediate PMMA surface layer no. 1. It is interesting to note that the resonant maxima in attenuation shown in Figures 5 and 7 occur for the same value of the product (frequency · thickness), that is for $fh_1 \approx 280$ MHz µm in Figure 5 and $fh_2 \approx 280$ MHz µm in Figure 7.

It is noteworthy that the problem of propagation of Love surface waves in multilayered lossy composite waveguides loaded with a viscoelastic Newtonian liquid can be formulated in terms of a direct Sturm–Liouville problem (Arfken and Weber, 2005). This suggests that Love surface waves propagating in lossy multilayered composite waveguides may have some analogies in electromagnetism and quantum mechanics (Malischewsky, 2009), where the formalism of the direct Sturm–Liouville problem is widely used.

6. Conclusions

Taking into account the results of the theoretical analysis and numerical calculations performed in this article, we can draw the following conclusions:

1. High viscosity η of the loading Newtonian liquid has in general a stiffening effect on Love wave composite waveguides. As a result, phase velocity v_p of Love waves increases as a function of frequencies for high viscosities ($\eta = 10$ Pa s) of the loading Newtonian liquid, see Figure 2
2. Attenuation α of Love waves exhibits resonant-like maxima, as a function of thickness h_1 of the first PMMA surface layer and a function of thickness h_2 of the second surface layer (Au), with an amplitude proportional to $\sqrt{\eta}$, see Figure 5
3. Attenuation α of Love waves exhibits resonant-like maxima, as a function of thickness h_2 of the second surface layer (Au), with an amplitude proportional to $\sqrt{\eta}$, see Figure 7
4. Resonant-like maxima in attenuation α of Love waves, as a function of thickness h_2 of the second

lossless elastic (Au) surface layer, occur, despite the fact that the second gold surface layer is not in direct contact with a lossy Newtonian liquid (see Figure 7).

The new wave phenomena enumerated in points 1–4 above occur only in Love wave waveguides with losses. They are entirely absent in lossless waveguides.

The results of theoretical analysis and numerical calculations, presented in this article, can be useful in NDT of layered lossy composite materials, mechanics of materials, as well as in designing and optimization of biosensors and chemosensors that use surface waves of the Love type. Similarly, the results of this work can find applications in geophysics and seismology as well as in mining and petroleum engineering.

Declaration of conflicting interests

The author(s) declared no potential conflicts of interest with respect to the research, authorship, and/or publication of this article.

Funding

The author(s) disclosed receipt of the following financial support for the research, authorship, and/or publication of this article: The project was funded by the National Science Centre (Poland), granted on the basis of Decision No. 2016/21/B/ST8/02437.

ORCID iD

Kiełczyński Piotr https://orcid.org/0000-0003-3909-342X

References

Achenbach JD (1973) *Wave Propagation in Elastic Solids*. Amsterdam: North-Holland.

Arfken GB and Weber HJ (2005) *Mathematical Methods for Physicists*. Amsterdam: Elsevier, Chap. 10.

Auld BA (1990) *Acoustic Fields and Waves in Solids*. Florida: Krieger Publishing Company, Vol. II.

Chattopadhyay A, Gupta S, Sharma VK, et al. (2010) Propagation of shear waves in viscoelastic medium at irregular boundaries. *Acta Geophysica* 58: 195–214.

Guo FL and Sun R (2008) Propagation of Bleustein–Gulyaev wave in 6 mm piezoelectric materials loaded with viscous liquid. *International Journal of Solids and Structures* 45: 3699–3710.

Gutierrez-Lemini D (2014) *Engineering Viscoelasticity*. New York: Springer.

Haskell NA (1953) The dispersion of surface waves on multilayered media. *Bulletin of the Seismological Society of America* 43: 17–34.

Kakar R and Kakar S (2012) Propagation of Love waves in a non-homogeneous elastic media. *Journal of Academia and Industrial Research* 1: 323–328.

Ke G, H Dong, Kristensen A, et al. (2011) Modified Thomson–Haskell matrix methods for surface-wave dispersion-curve calculation and their accelerated root-searching schemes. *Bulletin of the Seismological Society of America* 101: 1692–1703.

Kiełczyński P (1997) Attenuation of Love waves in low-loss media. *Journal of Applied Physics* 82: 5932–5937.

Kiełczyński P and Szalewski M (2011) An inverse method for determining the elastic properties of thin layers using Love surface waves. *Inverse Problems in Science and Engineering* 19: 31–43.

Kiełczyński P, Szalewski M and Balcerzak A (2012) Effect of viscous loading on Love wave propagation. *International Journal of Solids and Structures* 49: 2314–2319.

Kiełczyński P, Szalewski M and Balcerzak A (2014) Inverse procedure for simultaneous evaluation of viscosity and density of Newtonian liquids from dispersion curves of Love waves. *Journal of Applied Physics* 116: 044902.

Kiełczyński P, Szalewski M, Balcerzak A, et al. (2015) Group and phase velocity of Love waves propagating in elastic functionally graded materials. *Archives of Acoustics* 40: 273–281.

Kiełczyński P, Szalewski M, Balcerzak A, et al. (2016) Propagation of ultrasonic Love waves in nonhomogeneous elastic functionally graded materials. *Ultrasonics* 65: 220–227.

Kiełczyński P (2018) Surface Love waves in a lossy layered planar waveguide with a viscoelastic guiding layer. *Applied Mathematical Modelling* 53: 419–432.

Kundu S, Gupta S, Vaishnav PK, et al. (2014) Propagation of Love waves in a heterogeneous medium over an inhomogeneous half-space under the effect of point source. *Journal of Vibration and Control* 22: 1380–1391.

Malischewsky PG (2009) Connections between seismology, waveguide physics and quantum mechanics. In: Proceedings of the international conference *Days on diffraction*, Saint Petersburg, Russia, 26–29 May 2009, pp 144–150.

Rose JL (2014) *Ultrasonic Guided Waves in Solid Media*. Cambridge: Cambridge University Press.

Royer D and Dieulesaint E (2000) *Elastic Waves in Solids*. Berlin: Springer.

Sharma V and Kumar S (2017) Dispersion of SH waves in a viscoelastic layer imperfectly bonded with a couple stress substrate. *Journal of Theoretical and Applied Mechanics* 55: 535–546.

Singh SS (2010) Love wave at a layer medium bounded by irregular boundary surfaces. *Journal of Vibration and Control* 17(5): 789–795.

Thomson WT (1950) Transmission of elastic waves through a stratified solid medium. *Journal of Applied Physics* 21: 89–93.

Yuan S, Chen X and Zhan Z (2019) Analysis of attenuation and dispersion of Love wave in viscoelastic media by finite-difference modeling. *Geophysical Research Abstracts* 21: 21: EGU2019-13630-2.